Author(s): Čolović, P.; Szilner, S.; Illana, A.; Valiente-Dobón, J. J.; Corradi, L.; Pollarolo, G.; Mijatović, T.; Goasduff, A.; Benzoni, G.; Borge, M. J. G.; Boso, A.; Boukhari, A.; Ceruti, S.; Cubiss, J. G.; de Angelis, G.; De Witte, H.; Fioretto, E.; Fransen, Ch.; Galtarossa, F.; Gaffney, L. P.; Giannopoulos, E.; Hess, H.; Jurado-Gomez, M. L.; Kaya, L.; Kröll, Th.; Marchi, T.; Menegazzo, R.; Mengoni, D.; Napoli, D. R.; O'Neill,

Title: Population of lead isotopes in binary reactions using a 94Rb radioactive beam

Year: 2020

Version: Published version

Please cite the original version:

Čolović, P., Szilner, S., Illana, A., Valiente-Dobón, J.J., Corradi, L., Pollarolo, G., Mijatović, T., Goasduff, A., Benzoni, G., Borge, M. J. G., Boso, A., Boukhari, A., Ceruti, S., Cubiss, J. G., de Angelis, G., De Witte, H., Fioretto, E., Fransen, Ch., Galtarossa, F., . . . Zidarova, R. (2020). Population of lead isotopes in binary reactions using a 94Rb radioactive beam. Physical Review C, 102(5), Article 054609. https://doi.org/10.1103/physrevc.102.054609

Population of lead isotopes in binary reactions using a ^{94}Rb radioactive beam

P. Čolović,[1] S. Szilner,[1,*] A. Illana,[2] J. J. Valiente-Dobón,[2,†] L. Corradi,[2] G. Pollarolo,[3] T. Mijatović,[1] A. Goasduff,[2,4] G. Benzoni,[5] M. J. G. Borge,[6] A. Boso,[4] A. Boukhari,[7] S. Ceruti,[5] J. G. Cubiss,[8] G. de Angelis,[2] H. De Witte,[9] E. Fioretto,[2] Ch. Fransen,[10] F. Galtarossa,[2,11] L. P. Gaffney,[12,13] E. Giannopoulos,[12,14] H. Hess,[10] M. L. Jurado-Gomez,[15] L. Kaya,[10] Th. Kröll,[16] T. Marchi,[2] R. Menegazzo,[4] D. Mengoni,[4] D. R. Napoli,[2] G. O'Neill,[17] J. Pakarinen,[14] Zs. Podolyák,[18] F. Recchia,[4] P. Reiter,[10] D. Rosiak,[10] J. Snall,[12,19] P. Spagnoletti,[20] D. Testov,[4] S. Thiel,[10] N. Warr,[10] and R. Zidarova[14]

[1]*Ruder Bošković Institute Zagreb, Croatia*
[2]*Istituto Nazionale di Fisica Nucleare, Laboratori Nazionali di Legnaro, Legnaro, Italy*
[3]*Dipartimento di Fisica, Università di Torino, and Istituto Nazionale di Fisica Nucleare, Torino, Italy*
[4]*Dipartimento di Fisica, Università di Padova, and Istituto Nazionale di Fisica Nucleare, Padova, Italy*
[5]*Universitá degli Studi di Milano and INFN, Sezione di Milano, Milano, Italy*
[6]*Instituto de Estructura de la Materia, CSIC, Madrid, Spain*
[7]*University of Paris-Sud 11, Paris, France*
[8]*Department of Physics, University of York, York, United Kingdom*
[9]*Katholieke Universiteit, Leuven, Belgium*
[10]*Institut für Kernphysik, Universität zu Köln, Köln, Germany*
[11]*Université Paris-Saclay, CNRS/IN2P3, Orsay, France*
[12]*ISOLDE, CERN, Switzerland*
[13]*University of Liverpool, Liverpool, United Kingdom*
[14]*Department of Physics, University of Jyväskylä, Jyväskylä, Finland*
[15]*Instituto de Física Corpuscular CSIC, Valencia, Spain*
[16]*Institut für Kernphysik, Technische Universität Darmstadt, Darmstadt, Germany*
[17]*University of the Western Cape, Bellville, and iThemba Laboratory, South Africa*
[18]*Department of Physics, University of Surrey, Guildford, United Kingdom*
[19]*Lund University, Box 118, Lund, Sweden*
[20]*University of the West of Scotland, Paisley, United Kingdom*

(Received 15 September 2020; accepted 28 October 2020; published 19 November 2020)

We measured absolute cross sections for neutron transfer channels populated in the ^{94}Rb + ^{208}Pb binary reaction. Cross sections have been extracted identifying directly the lead isotopes with the high efficiency MINIBALL γ-ray array coupled to a particle detector combined with a radioactive ^{94}Rb beam delivered at $E_{\rm lab} = 6.2$ MeV/nucleon by the HIE-ISOLDE facility. We observed sizable cross sections in the neutron-rich mass region, where the heavy partner acquires neutrons. A fair agreement between the measured cross sections with those from GRAZING calculations gives confidence in the cross-section predictions of more neutron-rich nuclei produced via a larger number of transferred nucleons.

DOI: 10.1103/PhysRevC.102.054609

I. INTRODUCTION

Due to the growing availability of radioactive beams with suitable intensities there is presently an increasing interest in the study of reaction mechanisms which favor the production of neutron-rich heavy nuclei. The region of lead is particularly attractive since it lies near the $N = 126$ shell closure and is therefore strongly connected to the path of heavy-element synthesis [1]. To populate heavy neutron-rich nuclei, multinucleon transfer reactions between heavy ions is recognized as a very suitable mechanism [2–5]. Recently developed models predict large primary cross sections exploiting reactions at energies close to the Coulomb barrier. In this low-energy regime, multinucleon transfer reactions are mainly governed by optimum Q-value considerations and nuclear form factors [4]. The balance of Q values is mostly controlled by the light partner, and with stable nuclei the dominant processes are the neutron pick-up and the proton stripping from the light partner of the reaction. At the same time, the heavy reaction partner gains charge while losing neutrons. This has been confirmed in different high-resolution experiments, and

*Suzana.Szilner@irb.hr
†Javier.Valiente@lnl.infn.it

among those having ^{208}Pb as the reference target, in the reactions ^{32}S + ^{208}Pb [6], ^{40}Ca + ^{208}Pb [7], ^{58}Ni + ^{208}Pb [8], and ^{90}Zr + ^{208}Pb [9], encompassing projectiles in a wide mass range and with different structure properties.

With neutron-rich projectiles a change occurs in the population pattern of the light partner, where neutron stripping and proton pick-up channels open up. These channels are interesting since the correlated heavy partner of the reaction acquires neutrons while losing protons. With stable beams, the onset of such a population change has been observed in the reactions ^{64}Ni + ^{238}U [10], ^{40}Ar + ^{208}Pb [11], ^{136}Xe + ^{198}Pt [12], ^{136}Xe + ^{238}U [13], and ^{197}Au + ^{130}Te [14], detecting the light partners with magnetic spectrometers, and in the reactions ^{204}Hg + ^{198}Pt [15] and ^{136}Xe + ^{198}Pt [12], identifying also the heavy partners using γ-ray spectroscopy techniques.

The particular isotope of each element in the nuclear chart where the transition from one regime to the other occurs has been identified by systematic calculations of low-energy direct reactions [2]. These isotopes turn out to be somewhere between five to seven neutrons away from the last stable ones, highlighting the importance of the use of neutron-rich projectiles significantly far from stability. To properly test these predictions is a difficult task because it requires the identification of heavy reaction partners by their mass and charge after production with low-intensity radioactive ions.

This article reports the results of an experiment aiming to directly identify lead isotopes and determine their absolute cross sections by employing the high-efficiency MINIBALL γ-ray array [16] coupled to a particle detector [17], combined with a radioactive ^{94}Rb beam in the ^{94}Rb + ^{208}Pb binary reaction. The choice of the medium-mass ^{94}Rb beam ensured quite large primary cross sections. At the same time, the relatively low bombarding energy (in the vicinity of the Coulomb barrier and well suited to the upgraded HIE-ISOLDE facility), limits secondary processes, i.e., neutron evaporation and fission, which can significantly modify the final mass distributions.

In this work, we focus on pure neutron transfer channels, which are the most reliable ones for a quantitative comparison with theory. In fact, in neutron transfer processes the modification in the trajectories of entrance and exit channels is minimal, and the nuclear form factors are better known. This is the main reason why calculations describe the experimental cross sections extracted in measurements with stable beams particularly well (see Ref. [11] and references therein).

II. THE SETUP AND THE EXPERIMENT

A ^{94}Rb ion beam was delivered by the HIE-ISOLDE facility [18,19] in CERN onto a 1-mg/cm^2-thick ^{208}Pb target with a 99.6% isotopic enrichment. To produce ^{94}Rb, a 1.4-GeV proton beam from the PS-Booster was impinged on a uranium carbide target. The rubidium atoms then effuse out of the hot target and are ionized in a hot cavity ion source. The ^{94}Rb^{1+} ions were then extracted and mass separated by the general purpose separator. The average proton current was limited to $\approx$0.5 μA with an intensity of 1.2×10^{10} protons per pulse due to the dose rate experienced inside the experimental hall. To accelerate the beam to the final energy rubidium ions were injected into the Penning trap (REX-TRAP) [20] to cool and bunch the beam, before further charge breeding to ^{94}Rb^{23+} with a total breeding time of 123 ms [21]. The highly charged ions were injected into the REX linear accelerator and further accelerated in the new HIE-ISOLDE superconducting linear accelerator [19] up to $E_{\rm lab} = 6.2$ MeV/nucleon. In the center of the target, the bombarding energy corresponds to a value $\approx$30% higher than the Coulomb barrier, as a compromise between having rather large primary cross sections and limiting secondary processes. The beam had an intensity on target of 10^6 particles/s and a purity of $\approx$90% (with $\approx$10% of ^{94}Sr isobar). The high-resolution MINIBALL γ-ray spectrometer [16] coupled to an annular position sensitive silicon detector [17] allowed the identification of reaction products via their associated γ rays. MINIBALL comprises 24 high-purity germanium crystals, individually encapsulated in triple-cluster cryostats which surround a spherical target chamber in compact geometry [16]. The absolute efficiency was $\approx$8% for a 1.3 MeV γ ray, with position sensitivity obtained via six-fold electrical segmentation of each crystal electrode. Binary products were detected by four particle detectors of DSSSD-type (double-sided silicon strip detectors), each one made of 16 annular strips spanning a scattering angular range $\theta_{\rm lab} = 24^\circ$–$63^\circ$. At the chosen bombarding energy this geometry allowed most of the total transfer flux to be collected (when tagging on Rb-like ions).

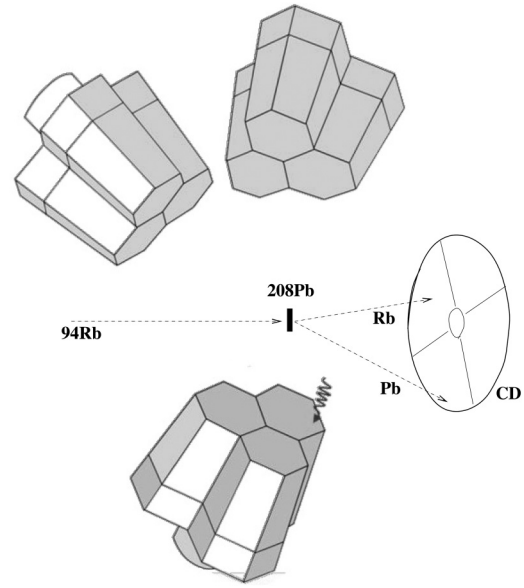

FIG. 1. Layout of the setup used in the study of the ^{94}Rb + ^{208}Pb reaction, with schematic representation of the MINIBALL cluster detectors (eight clusters were used), and the silicon CD configuration.

The detectors were arranged in a close geometry with the compact-disk-shaped (CD-shaped) particle detector at forward angles, symmetrically arranged around the beam axis at a central distance of 21 mm downstream relative to the target. Figure 1 shows a scheme of the setup. The CD detector provided position (angle) and energy information. In addition, a timing signal was used to construct the time-of-flight between particles and associated γ rays. This last information allowed separation of the prompt γ rays (up to 200 ns) from

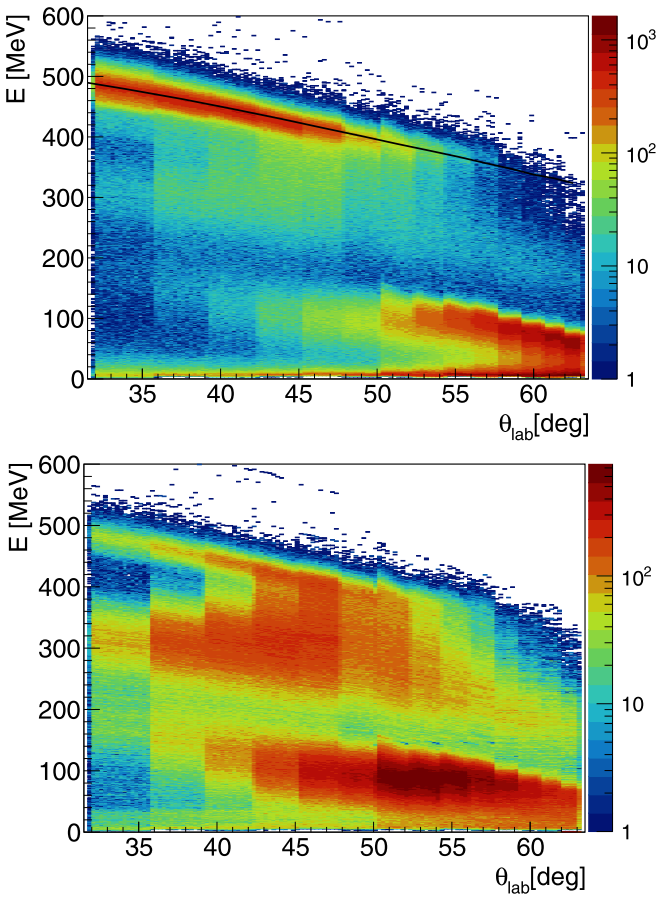

FIG. 2. (top) Matrix of total kinetic energy vs angle for the measured ^{94}Rb + ^{208}Pb reaction. The upper and lower bands correspond to Rb-like and Pb-like ions, respectively. The black line indicates Rutherford scattering. (bottom) Same matrix of total kinetic energy vs angle in coincidence with γ rays.

the delayed ones and to perform a background subtraction. The delayed part of the spectrum was also used to evaluate the decay yields of isomeric states (see below).

In these kind of binary reactions it is important to have as complete a view as possible of the characteristics of the process. At energies slightly above the Coulomb barrier angular distributions are bell shaped and centered at the grazing angle. Moreover, quasi-elastic and deep-inelastic processes partially overlap, with kinetic-energy distributions depending on the scattering angle. To visualize the whole reaction, two-dimensional matrices of energy E vs scattering angle $\theta_{\rm lab}$ (Wilczynski plots) are shown for the presently studied system in Fig. 2 (top). One sees a very clear separation between the beam-like and target-like fragments. In the upper part of the figure, the main "band" of the Rb-like events follows the behavior of quasi-elastic processes, as seen also from the superimposed calculated Rutherford scattering. In the lower part of the figure the Pb-like events, due to binary kinematics, cover a different kinematical angular range. One also sees that the Rb events undergo a bending towards much lower kinetic energies, corresponding to dissipative processes (see region close to $\theta_{\rm lab} \approx 47^\circ$). This behavior is more clear in the same matrix, shown in the bottom part of Fig. 2, but constructed with the condition of coincidence with γ rays. Evidently, the intensity of the event distribution is higher in the region of large energy loss, that being the region associated with higher excitation energy and larger γ-ray multiplicities of the binary products.

To construct the coincident γ-ray spectra we selected the regions of the E-$\theta_{\rm lab}$ matrix corresponding to quasi-elastic processes. This was done in order to extract the yields of the transfer channels as close to the grazing regime as possible, i.e., with small energy loss, which helped in optimizing the Doppler correction of the γ rays. In fact, since γ rays were emitted in flight, Doppler corrections had to be applied for both the Rb-like and Pb-like fragments using the position information from the CD detector. The Rb-like events were kept as a reference in the analysis, since they cover most of the transfer angular distribution. In this way, while the Doppler correction for Rb-like events was applied directly, the one for Pb-like ions was done by assuming binary kinematics and almost pure Rutherford scattering. With a velocity of the Pb-like fragments $\beta \approx 5\%$, a final resolution of 1.2% at 1.5 MeV was achieved. Figure 3 (top panel) shows the Doppler-corrected spectrum for the Pb-like ions, where one observes the main γ-ray transitions associated with the inelastic channel (^{208}Pb) and with the neutron pick-up and stripping transfer channels (^{207,209,210}Pb). The bottom panel of the same figure displays the delayed part of the spectrum relevant for the analysis of the isomeric decay of ^{210}Pb (see below). For the sake of completeness we mention that, in the spectrum Doppler corrected for the Rb-like ions, we were able to observe the main γ-ray transitions of the populated Rb isotopes, which are, however, associated with more complex and less known level schemes than for Pb.

III. DATA ANALYSIS AND DISCUSSION

A. Determination of absolute cross sections

To get the absolute value of the cross sections, we have taken as a reference the lowest 3^- octupole state of ^{208}Pb and normalized its intensity at forward angles to a distorted-wave Born approximation (DWBA) carried out at a bombarding energy $E_{\rm lab} = 575$ MeV, corresponding to the center of the ^{208}Pb target.

To extract the experimental angular distribution of the 3^- state, the dominant feeding from above needs to be taken into account. To achieve this, we subtracted the angular distribution of $E_\gamma = 583$ keV ($5^- \rightarrow 3^-$) from the one of $E_\gamma = 2615$ keV ($3^- \rightarrow 0^+$). For the final experimental angular distribution of the 3^- state we integrated the subtracted γ intensity in bins of $\Delta\theta_{\rm lab} = 3.12^\circ$ for the coincident particle in the CD detector. Such a procedure has been carried out for the whole angular range of the Rb-like ions (see also Fig. 2). The data are shown in the upper part of Fig. 4 together with the DWBA calculations. Calculations were performed with the code PTOLEMY [23] by using the standard optical potential and tabulated values. For completeness, in the bottom part of Fig. 4 we show also the corresponding elastic scattering in comparison with the extracted quasi-elastic data (divided by the Rutherford cross section). The experimental points

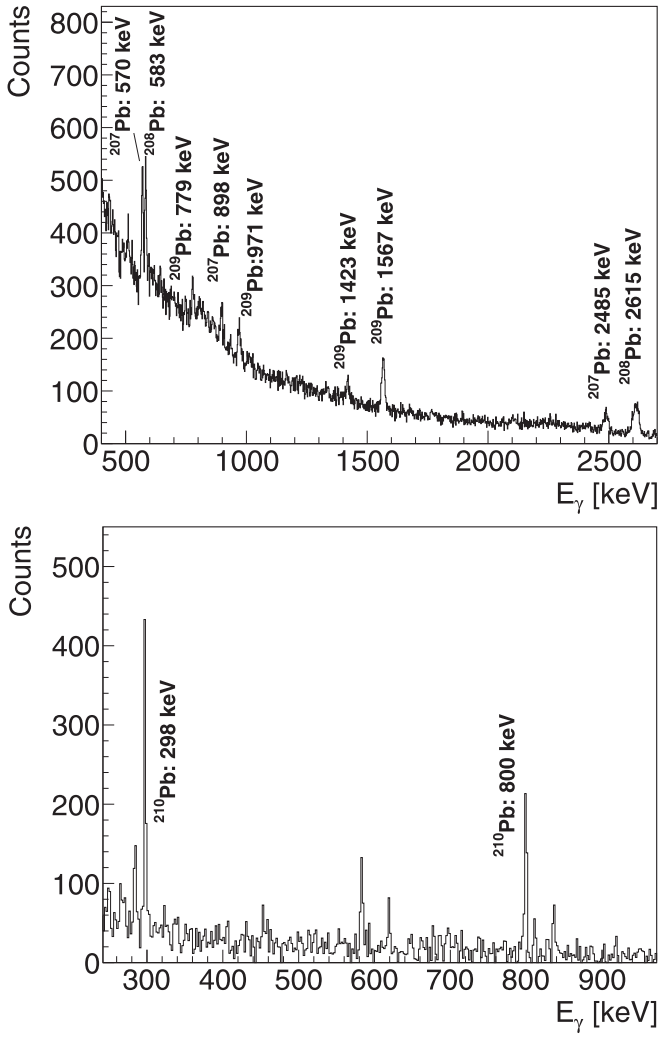

FIG. 3. Prompt, up to 200 ns (top), and delayed, up to 2μs (bottom) γ-ray spectra taken in coincidence with the Rb-like detected in CD detector, in the selected energy ranges. The observed γ-ray transitions associated with the populated isotopes of Pb are labeled.

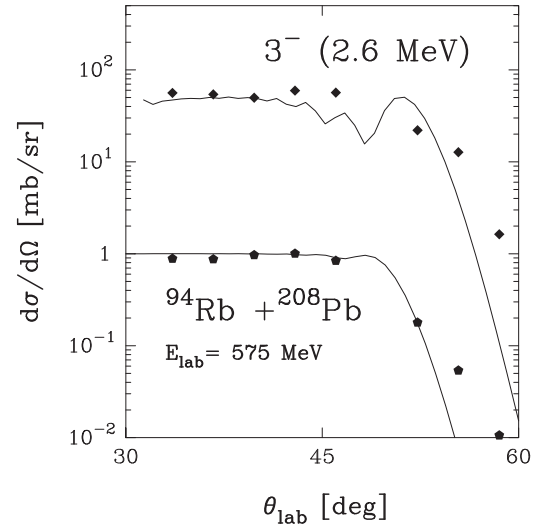

FIG. 4. (top) Experimental (diamonds) and theoretical (line) differential cross sections for the inelastic scattering of the 3^- state in ^{208}Pb. Data have been normalized at forward angles to the DWBA calculation at $E_{lab} = 575$ MeV. Recall that the experimental points correspond to an integration in bins $\theta_{lab} = 3.12^\circ$. (bottom) Experimental quasi-elastic cross sections (pentagons) and theoretical elastic scattering (line), divided by Rutherford cross section.

start to deviate from the pure Rutherford scattering in the angular region where the inelastic scattering exhibits the main oscillation pattern.

With the shown normalization procedure we extracted a factor to convert the γ yields into cross sections, and that factor was kept the same for all of the observed transfer channels. With the structure information of Rb isotopes being less known, in the following we concentrate only on the quantitative analysis of Pb isotopes, which are the heavy partners of the reaction and the main object of the present work.

In Fig. 5 we display the level scheme of ^{207,208,209,210}Pb isotopes, corresponding to all transfer channels we could observe in the experiment. For the one-neutron transfers, we expect that the strongest populated states are those of single-particle character. In ^{207}Pb these states are associated with the sequence of orbitals $d_{5/2}$, $p_{3/2}$, $i_{13/2}$, $f_{7/2}$, and $h_{9/2}$ in the $N = 82$–126 shell. We indeed saw that the γ-ray decays from the states $5/2^-$ ($E_\gamma = 570$ keV), $3/2^-$ ($E_\gamma = 898$ keV) and $7/2^-$ ($E_\gamma = 1770$ keV). The $13/2^+$ state is an isomer ($T_{1/2} = 0.8$ s) and its decay could not be observed. However, the feeding from above was taken into account in the extraction of the total cross section. In ^{209}Pb we expect to populate the $9/2^+$, $11/2^+$, $15/2^-$, $5/2^+$, $1/2^+$, $7/2^+$, and $3/2^+$ states, where the unpaired neutron occupies the $g_{9/2}$, $i_{11/2}$, $j_{15/2}$, $d_{5/2}$, $s_{1/2}$, $g_{7/2}$, and $d_{3/2}$ orbitals. In fact, we observed the decays from these states. For both ^{207}Pb and ^{209}Pb the cross sections were obtained by adding the intensities of all the observed γ rays which were not in cascade. For the even-even ^{210}Pb the level scheme is rather simple with all decays passing through the first 2^+ state, whose decay strength to the 0^+ ground state could be safely determined. However we have to take into account that part of the transfer flux feeds the 6^+ and 8^+ isomeric states. Their contribution to the cross sections has been extracted by adding the γ yield from the decay of the 2^+ state corresponding to the delayed part of the time-of-flight spectrum between the CD and γ-array detectors (see also Fig. 3, bottom panel). We remark that we do not clearly observe the population of ^{206}Pb, even if the predicted cross section of this channel is approximately half of the ^{210}Pb one. In fact, in ^{206}Pb, the lowest negative-parity state is an isomer with a half-life of 125 μs, which falls completely outside our timing gate.

B. Estimates of the ground-state cross sections of Pb isotopes

Of course, by integrating all γ intensity associated with each specific isotope of lead we extract a lower limit for the cross sections because we are missing at least the ground-state population. Thus we tried to estimate such a population. For ^{207}Pb we compared the population strength observed in the present experiment with those of reactions with other heavy ions at a similar bombarding energy range close to the

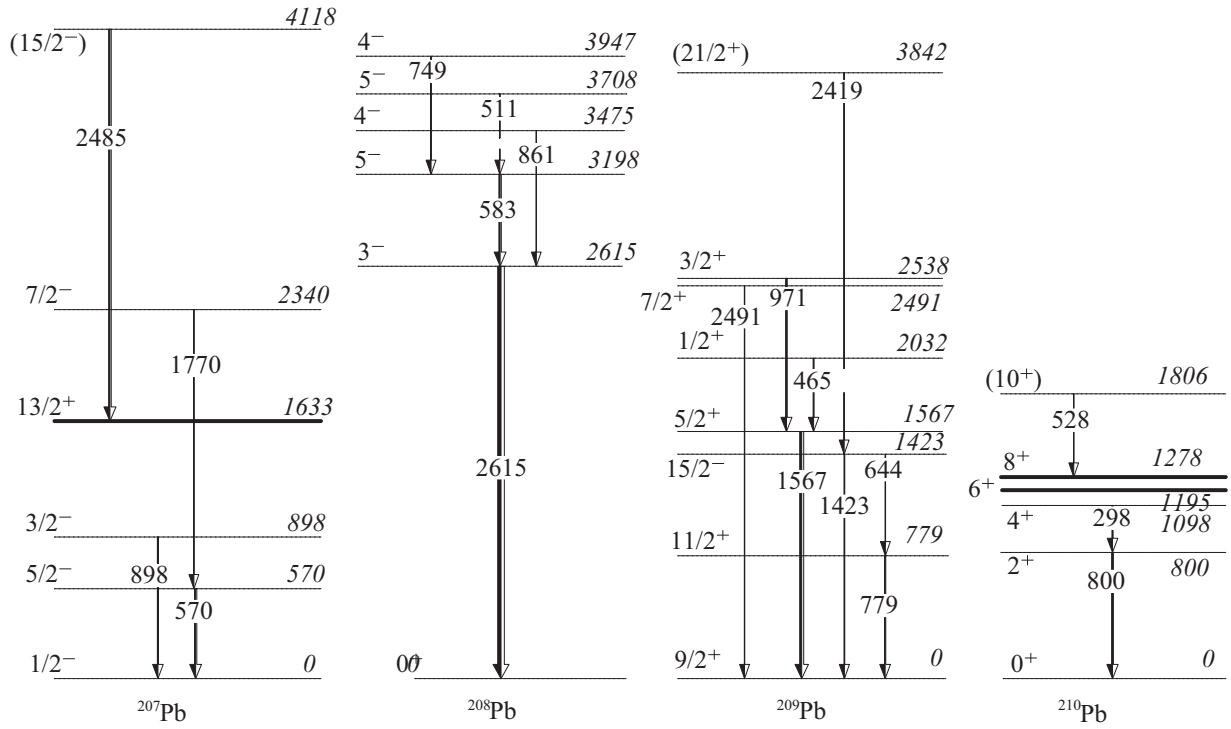

FIG. 5. Level scheme of ^{207,208,209,210}Pb isotopes. Relative γ-ray intensities are indicated by the width of the arrows. Only prompt transitions observed in our measurements are plotted. The energy, spin, and parity of levels, their branching ratios and energy of transitions are as in Ref. [22]. The levels represented by a thicker line correspond to isomers.

Coulomb barrier and having ^{208}Pb as target. This comparison is shown in Fig. 6 for the ^{94}Rb + ^{208}Pb, ^{90}Zr + ^{208}Pb [24], ^{40}Ar + ^{208}Pb, and ^{32}S + ^{208}Pb [25] transfer reactions. One sees that the intensity distributions among the lowest excited states are rather similar. This fact should reflect a convolution of Q-value arguments and structure properties. The ground-state Q values for the one-neutron transfer channels are very much alike and within few MeV for all the shown systems. Therefore, the transfer flux is governed by similar Q-value windows (recall that, for neutron transfer channels, the optimum Q-value window is centered at ≈0 MeV and has a width of a few MeV). From the structural point of view one expects that the strongest populated states in the one-neutron transfer channels will be those of single-particle character. In light-ion-induced reactions, in particular in the ^{208}Pb$(p,d)^{207}$Pb reactions [22], the spectroscopic factors for the three lowest lying $1/2^-$, $5/2^-$, and $3/2^-$ states, indicate their dominant configuration with a hole in the $p_{1/2}$, $d_{5/2}$, and $p_{3/2}$ orbitals. The same is true for the two lowest $9/2^+$ and $11/2^+$ states in ^{209}Pb where again the $g_{9/2}$ and $i_{11/2}$ spectroscopic factors show little fragmentation. Thus, by taking into account the strong single-particle character of these states and the fact that they differ only slightly in excitation energy (<1 MeV) and spin, one can expect that they are populated with similar strength.

Based on these arguments we quoted the ground-state population for ^{207}Pb ($1/2^-$ state) as the average of those for its first $5/2^-$ and $3/2^-$ states. For ^{209}Pb, although in this case heavy-ion data are more scarce, we followed a similar procedure, keeping the ground-state population ($9/2^+$ state) the same as for the first excited $11/2^+$ state.

To estimate the ground-state population of ^{208}Pb and ^{210}Pb we extracted the direct feeding of the 3^- and 2^+ states, respectively, and we assumed that their corresponding cross sections equals those of their ground states. This rather modest estimation of the ground-state cross sections was corroborated with an additional analysis of the previously measured ^{40}Ar + ^{208}Pb reaction. In this reaction, differential and total cross sections of the different transfer channels were extracted by employing the PRISMA magnetic spectrometer coupled to the CLARA γ-ray array [11]. To get the absolute value of the cross section to excited states, we normalized the intensity of the 3^- state in ^{208}Pb to DWBA calculations by using a procedure similar to the one presented in this work. The comparison of the cross sections measured with CLARA with the total absolute cross section measured with PRISMA [26] determines the proportion of the ground-state cross sections with respect to the total cross sections.

C. Comparison with GRAZING calculations

The experimental cross sections for the Pb isotopes deduced in the way described in the previous section are reported in Fig. 7, along with the values corresponding to the γ yields directly extracted from the experiment (lower bars) and those where the estimated cross sections to the ground states of Pb isotopes have been added (points). The former values have to be considered as lower limits for the cross sections. The

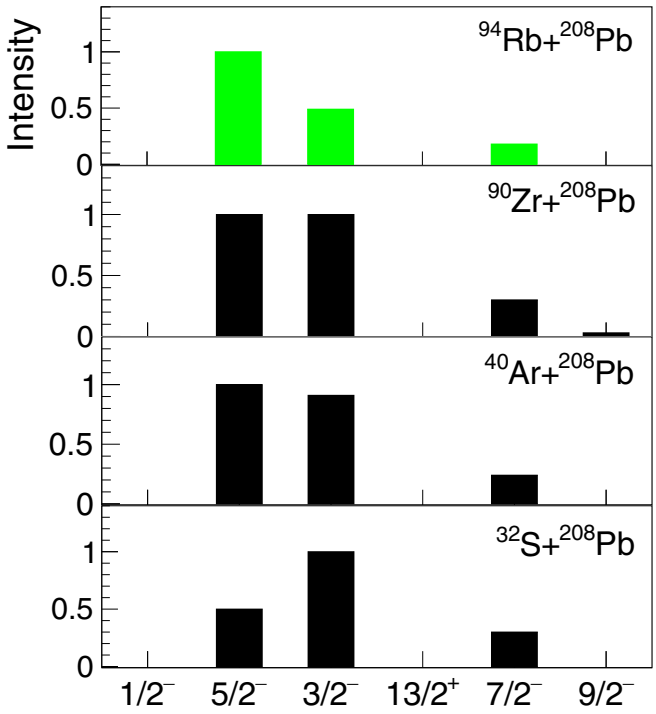

FIG. 6. Intensity of different states in ^{207}Pb, normalized to the strongest transitions, populated in the ^{94}Rb + ^{208}Pb, ^{90}Zr + ^{208}Pb [24], ^{40}Ar + ^{208}Pb, and ^{32}S + ^{208}Pb [25] transfer reactions.

latter, incorporating indirect estimates, should also contain the contribution of the Rb partners, assuming negligible mutual excitation.

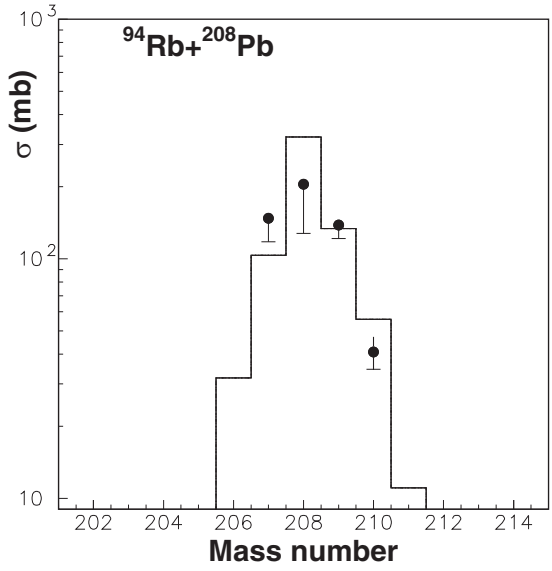

FIG. 7. Total cross sections of Pb isotopes. The measured cross sections are indicated as lower limits, while those which include the estimated values for the ground states are indicated with full points. The histogram is the GRAZING prediction for $E_{\rm lab} = 575$ MeV, the same as that for the DWBA calculations shown in Fig. 4.

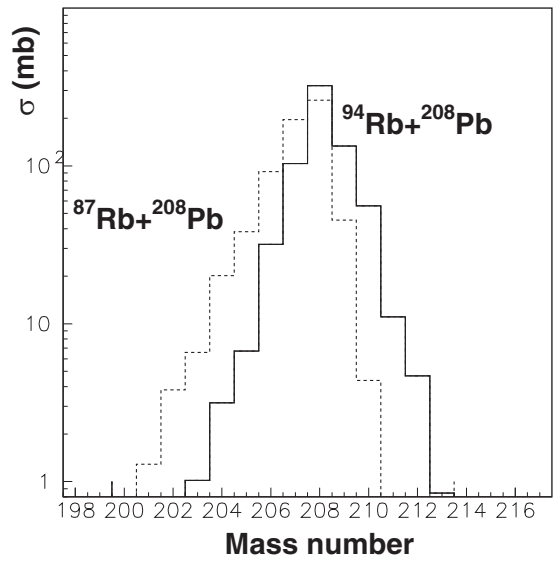

FIG. 8. GRAZING calculated total cross sections for Pb isotopes in ^{94}Rb + ^{208}Pb (full line) and ^{87}Rb + ^{208}Pb (dashed line) reactions at $E_{\rm lab} = 575$ MeV.

Data have been compared with calculations performed by the GRAZING model [27–29]. This model calculates the evolution of the reaction by taking into account, besides the relative motion variables, the intrinsic degrees of freedom of projectile and target. These are the surface degrees of freedom and the one-nucleon transfer channels. The relative motion of the system is calculated in a nuclear plus Coulomb field. The exchange of many nucleons proceeds via a multistep mechanism of single nucleons. This model has been so far successfully applied in the description of multinucleon transfer reactions as well as of fusion reactions. In particular, the model turned out to describe well the experimental neutron transfer cross sections for a large amount of data sets taken in reactions with stable beams (see Refs. [4,11] and references therein). Therefore, this represents a good basis to judge the quality of agreement with data for reactions involving nuclei far from stability, and to confirm the transition to the regime where the heavy partner acquires neutrons while loosing protons, discussed in the introduction.

In Fig. 7 we show the GRAZING predictions, taking into account neutron evaporation. One sees clearly the sizable cross sections in the neutron-rich mass region, which confirms the predicted change of population pattern. One also finds a rather fair agreement between the data and calculations. In the higher mass region, the experimental cross section for ^{209}Pb is particularly well reproduced. The values of the cross sections have their justification mainly in the optimum Q-value arguments discussed in Ref. [2]. To better illustrate this crucial point we show for comparison in Fig. 8 the corresponding calculated cross sections for the reaction using ^{87}Rb, the most neutron-rich stable isotope of Rb, which differs by seven neutrons from the presently employed ^{94}Rb. One clearly observes much lower values for the neutron-rich Pb isotopes and, reversely, much larger values for the neutron-poor isotopes. This follows from the fact that, with the ^{87}Rb projectile, channels

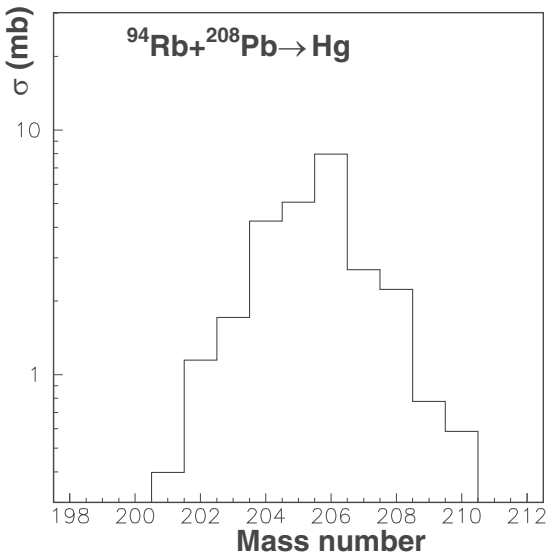

FIG. 9. GRAZING calculated total cross sections for Hg isotopes in the ^{94}Rb + ^{208}Pb reaction at $E_{\rm lab} = 575$ MeV.

corresponding to neutron pick-up (and proton stripping) from the light partner of the reaction are favored. For the same reason, the cross sections obtained with ^{94}Rb for the neutron rich heavy partners are orders of magnitudes larger than those with ^{87}Rb when considering proton pick-up channels.

These results give us confidence to predict the transfer cross sections for channels where larger number of nucleons are involved. As an example, we show in Fig. 9 the calculated cross sections for the Hg isotopes. In these nuclei the two protons removed from the $Z = 82$ core should act as spectators, thus encompassing the same neutron valence space as in Pb isotopes. The existence of moderately-high-spin isomers in this part of the nuclear landscape is attributed to a stretched configuration of the coupled valence neutrons. The population of such high-spin states will be favored by the transfer mechanism because it maximizes the transferred angular momentum [30,31]. One also expects a strong excitation of states connected with the surface degrees of freedom, relevant in the mechanism of the transfer of energy and angular momentum from the relative motion. Properties of such states serve as the first indication of shape changes. The sensitivity to study these states could be reached in experiments with beam intensities an order of magnitude larger than the present one, actually already achievable at radioactive beam facilities.

IV. SUMMARY AND OUTLOOK

Absolute cross sections for the population of lead isotopes have been measured in the ^{94}Rb + ^{208}Pb binary reaction using a neutron-rich ^{94}Rb radioactive beam at a bombarding energy ≈30% above the Coulomb barrier. The neutron transfer channels have been identified by means of the high-efficiency MINIBALL γ-ray array coupled to a particle detector. The data show sizable cross sections for the population of the neutron-rich mass region, confirming the theoretical predictions of the GRAZING code. A reasonable agreement with the experiment was found, giving us confidence for cross-section predictions of channels involving a larger number of nucleons and populating more neutron-rich regions. This is important for future studies of nuclear structure, in particular near the $N = 126$ shell closure, exploiting the unique possibilities offered by multinucleon transfer reactions. The present experiment has to be considered as first step in this direction.

ACKNOWLEDGMENTS

We acknowledge the support of the ISOLDE Collaboration and technical teams. The authors are grateful to the HIE-ISOLDE staff for the effort made in the production and acceleration of radioactive ^{94}Rb beam. The authors are grateful to the INFN-LNL target laboratory for the excellent targets. This work was partly supported by the HORIZON 2020 ENSAR2 Grant Agreement no. 654002, and Marie Skłodowska-Curie COFUND (EU-CERN) grant agreement no. 665779, and by STFC (U.K.). This work has been supported in part by the Croatian Science Foundation under Project no. 7194 and in part under Project no. IP-2018-01-1257, and the German BMBF under contract 05P18PKCIA + Verbundprojekt 05P2018.

[1] K.-L. Kratz, J.-P. Bitouzet, F.-K. Thielemann, P. Moeller, and B. Pfeiffer, Astrophys. J. **403**, 216 (1993).
[2] C. H. Dasso, G. Pollarolo, and A. Winther, Phys. Rev. Lett. **73**, 1907 (1994).
[3] V. Zagrebaev and W. Greiner, Phys. Rev. Lett. **101**, 122701 (2008).
[4] L. Corradi, G. Pollarolo, and S. Szilner, J. Phys. G **36**, 113101 (2009).
[5] K. Sekizawa, Front. Phys. **7**, 20 (2019).
[6] L. Corradi, A. M. Stefanini, D. Ackermann, S. Beghini, G. Montagnoli, C. Petrache, F. Scarlassara, C. H. Dasso, G. Pollarolo, and A. Winther, Phys. Rev. C **49**, R2875(R) (1994).
[7] S. Szilner, L. Corradi, G. Pollarolo, S. Beghini, B. R. Behera, E. Fioretto, A. Gadea, F. Haas, A. Latina, G. Montagnoli, F. Scarlassara, A. M. Stefanini, M. Trotta, A. M. Vinodkumar, and Y. Wu, Phys. Rev. C **71**, 044610 (2005).
[8] L. Corradi, A. M. Vinodkumar, A. M. Stefanini, E. Fioretto, G. Prete, S. Beghini, G. Montagnoli, F. Scarlassara, G. Pollarolo, F. Cerutti, and A. Winther, Phys. Rev. C **66**, 024606 (2002).
[9] S. Szilner, C. A. Ur, L. Corradi, N. Mărginean, G. Pollarolo, A. M. Stefanini, S. Beghini, B. R. Behera, E. Fioretto, A. Gadea, B. Guiot, A. Latina, P. Mason, G. Montagnoli, F. Scarlassara, M. Trotta, G. de Angelis, F. Della Vedova, E. Farnea, F. Haas *et al.*, Phys. Rev. C **76**, 024604 (2007).
[10] L. Corradi, A. M. Stefanini, C. J. Lin, S. Beghini, G. Montagnoli, F. Scarlassara, G. Pollarolo, and A. Winther, Phys. Rev. C **59**, 261 (1999).

[11] T. Mijatović, S. Szilner, L. Corradi, D. Montanari, G. Pollarolo, E. Fioretto, A. Gadea, A. Goasduff, D. Jelavić Malenica, N. Mărginean, M. Milin, G. Montagnoli, F. Scarlassara, N. Soić, A. M. Stefanini, C. A. Ur, and J. J. Valiente-Dobón, Phys. Rev. C **94**, 064616 (2016).
[12] Y. X. Watanabe, Y. H. Kim, S. C. Jeong, Y. Hirayama, N. Imai, H. Ishiyama, H. S. Jung, H. Miyatake, S. Choi, J. S. Song, E. Clement, G. de France, A. Navin, M. Rejmund, C. Schmitt, G. Pollarolo, L. Corradi, E. Fioretto, D. Montanari, M. Niikura *et al.*, Phys. Rev. Lett. **115**, 172503 (2015).
[13] A. Vogt, B. Birkenbach, P. Reiter, L. Corradi, T. Mijatović, D. Montanari, S. Szilner, D. Bazzacco, M. Bowry, A. Bracco, B. Bruyneel, F. C. L. Crespi, G. de Angelis, P. Désesquelles, J. Eberth, E. Farnea, E. Fioretto, A. Gadea, K. Geibel, A. Gengelbach *et al.*, Phys. Rev. C **92**, 024619 (2015).
[14] F. Galtarossa, L. Corradi, S. Szilner, E. Fioretto, G. Pollarolo, T. Mijatović, D. Montanari, D. Ackermann, D. Bourgin, S. Courtin, G. Fruet, A. Goasduff, J. Grebosz, F. Haas, D. Jelavić Malenica, S. C. Jeong, H. M. Jia, P. R. John, D. Mengoni, M. Milin *et al.*, Phys. Rev. C **97**, 054606 (2018).
[15] T. Welsh, W. Loveland, R. Yanez, J. S. Barrett, E. A. McCutchan, A. A. Sonzogni, T. Johnson, S. Zhu, J. P. Greene, A. D. Ayangeakaa, M. P. Carpenter, T. Lauritsen, J. L. Harker, W. B. Walters, B. M. S. Amro, and P. Copp, Phys. Lett. B **771**, 119 (2017).
[16] N. Warr *et al.*, Eur. Phys. J. A **49**, 40 (2013).
[17] A. N. Ostrowski *et al.*, Nucl. Instrum. Methods Phys. Res., Sect. A **480**, 448 (2002).
[18] M. J. G. Borge and K. Riisager, Eur. Phys. J. A **52**, 11 (2016).
[19] Y. Kadi, Y. Blumenfeld, W. V. Delsolaro, M. A. Fraser, M. Huyse, A. P. Koufidou, J. A. Rodriguez, and F. Wenander, J. Phys. G **44**, 084003 (2017).
[20] F. Ames, G. Bollen, P. Delahaye, O. Forstner, G. Huber, O. Kester, K. Reisinger, and P. Schmidt, Nucl. Instrum. Methods Phys. Res., Sect. A **538**, 17 (2005).
[21] F. Wenander, J. Instrum. **5**, C10004 (2010).
[22] F. G. Kondev and S. Lalkovski, Nucl. Data Sheets **112**, 707 (2011); M. J. Martin, *ibid.* **108**, 1583 (2007); J. Chen and F. G. Kondev, *ibid.* **126**, 373 (2015); M. Shamsuzzoha Basunia, *ibid.* **121**, 561 (2014).
[23] M. Rhoades-Brown, M. H. Macfarlane, and S. C. Pieper, Phys. Rev. C **21**, 2417 (1980);; **21**, 2436 (1980).
[24] M. V. Pajtler, Ph.D. thesis, Univeristy of Zagreb, 2014 (unpublished).
[25] L. Corradi, C. M. Petrache, D. Ackermann, S. Beghini, G. de Angelis, G. Montagnoli, H. Moreno, D. R. Napoli, G. Pollarolo, F. Scarlassara, G. F. Segato, C. Signorini, P. Spolaore, and A. M. Stefanini, Z. Phys. A: Hadrons Nucl. **344**, 353 (1992).
[26] K. Gorički, M. Sc. thesis, Faculty of Science, University of Zagreb, 2020 (unpublished).
[27] A. Winther, Nucl. Phys. A **572**, 191 (1994).
[28] A. Winther, Nucl. Phys. A **594**, 203 (1995).
[29] Program GRAZING, http:/www.to.infn.it/∼nanni/grazing.
[30] A. R. Barnett, W. R. Phillips, P. J. A. Buttle, and L. J. B. Goldfarb, Nucl. Phys. A **176**, 321 (1971).
[31] D. M. Brink, Phys. Lett. B **40**, 37 (1972).